



OPEN

Screening and predicting progression from high-risk mild cognitive impairment to Alzheimer's disease

Xiao-Yan Ge^{1,2}, Kai Cui², Long Liu¹, Yao Qin¹, Jing Cui¹, Hong-Juan Han³, Yan-Hong Luo¹ & Hong-Mei Yu^{1,4}✉

Individuals with mild cognitive impairment (MCI) are clinically heterogeneous, with different risks of progression to Alzheimer's disease. Regular follow-up and examination may be time-consuming and costly, especially for MRI and PET. Therefore, it is necessary to identify a more precise MRI population. In this study, a two-stage screening frame was proposed for evaluating the predictive utility of additional MRI measurements among high-risk MCI subjects. In the first stage, the K-means cluster was performed for trajectory-template based on two clinical assessments. In the second stage, high-risk individuals were filtered out and imputed into prognosis models with varying strategies. As a result, the ADAS-13 was more sensitive for filtering out high-risk individuals among patients with MCI. The optimal model included a change rate of clinical assessments and three neuroimaging measurements and was significantly associated with a net reclassification improvement (NRI) of 0.246 (95% CI 0.021, 0.848) and integrated discrimination improvement (IDI) of 0.090 (95% CI -0.062, 0.170). The ADAS-13 longitudinal models had the best discrimination performance (Optimism-corrected concordance index = 0.830), as validated by the bootstrap method. Considering the limited medical and financial resources, our findings recommend follow-up MRI examination 1 year after identification for high-risk individuals, while regular clinical assessments for low-risk individuals.

Alzheimer's disease (AD) is the most common cause of dementia in developing countries and is expected to affect 1 in 85 people worldwide by the year 2050¹. Mild cognitive impairment (MCI) is a transitional stage between normal cognition and dementia, and MCI patients are commonly enrolled as the target population for evaluating prognosis and early intervention for dementia^{2,3}. Moreover, individuals with MCI are clinically heterogeneous, with different risks of progression to AD⁴. Therefore, identifying patients with MCI who are at risk of progression to AD and improving the prognosis of MCI is of vital importance in the personalised clinical management of AD.

Existing studies have used multimodal information, including neurocognitive, magnetic resonance imaging (MRI), CSF-based, and positron emission tomography (PET) markers for binary classification modeling⁵⁻⁷. Although these studies have shown high classification accuracy, some approaches are often unavailable in the primary clinical setting, considering the cost and invasiveness of the procedures. Numerous convenient medical checks, such as neuropsychological tests, are preferred in primary screening⁸⁻¹⁰. Advanced examination technologies should be considered only when they are necessary for more precise diagnosis; otherwise, their value in the predictive model may be offset by their inconvenience. To maximise the value of these advanced detection methods and to reduce the burden on patients, it is necessary to focus on those at high risk of developing AD¹¹⁻¹⁴.

Additionally, many studies predicted the probability of conversion from MCI to AD as a binary response at a fixed time point (i.e., 3 years or 5 years), which did not consider the time interval during the conversion. Some studies used Cox regression models to investigate the time of the development from MCI to AD during follow-up¹⁵⁻¹⁷; however, most of these studies evaluated the predictive effect of single or combined prognostic markers only at the baseline¹⁸. In actual clinical practice, we often collect follow-up information on prognostic

¹Department of Health Statistics, School of Public Health, Shanxi Medical University, 56 XinJian South Road, Taiyuan, China. ²Department of Health Statistics, School of Public Health, Jinzhou Medical University, 40 SongPo Road, Jinzhou, China. ³Department of Mathematics, School of Basic Medical Sciences, Shanxi Medical University, Taiyuan, China. ⁴Shanxi Provincial Key Laboratory of Major Diseases Risk Assessment, 56 XinJian South Road, Taiyuan, China. ✉email: yu@sxmu.edu.cn

Characteristics	Mean (SD) or N (%)	
	Stage I: ADNI-1 (N = 85)	Stage II: ADNI GO/2 (N = 374)
Age (year)	74.2 (6.9)	71.2 (7.4)
Gender		
Male	61 (71.8)	206 (55.1)
Female	24 (28.2)	168 (44.9)
Marital status		
Married	73 (85.9)	278 (74.3)
Divorced	2 (2.4)	43 (11.5)
Others	10 (11.8)	53 (14.2)
Education		
Medium	0 (0.0)	2 (0.5)
High	85 (100.0)	372 (99.5)
ApoEε4		
Absent	36 (42.4)	199 (53.2)
Present	49 (57.7)	175 (46.8)
ADAS-13 Trajectory Label		
Low-risk	44 (51.8)	264 (70.6)
High-risk	41 (48.2)	110 (29.4)
MMSE Trajectory Label		
High-risk	50 (58.8)	92 (24.6)
Low-risk	35 (41.2)	282 (75.4)
ADAS-13_bl	30.3 (17.0)	14.5 (6.4)
MMSE_bl	27.5 (1.6)	28.1 (1.7)
CDRSB_bl	1.6 (0.9)	1.4 (0.9)
Total	85	374

Table 1. Baseline characteristics of subjects in two stages. ADAS-13, Alzheimer Disease Assessment Scale Cognitive 13 items; MMSE, mini mental state examination; ADAS-13_bl, Alzheimer Disease Assessment Scale Cognitive 13 items at Baseline; MMSE_bl, mini mental state examination at Baseline; CDRSB_bl, Clinical Dementia Rating Sum of Boxes at Baseline; SD, standard deviation.

markers, such as the cognitive assessment and MRI examinations. It is necessary to make full use of these follow-up information to predict the progression of MCI.

In the current study, we constructed a two-stage screening frame for individuals with MCI and evaluated the prognostic value of MRI in high-risk subjects with MCI. In stage I, we built the Alzheimer Disease Assessment Scale Cognitive 13 items (ADAS-13) and Mini Mental State Examination (MMSE) trajectory-templates of cognitive decline. In stage II, two trajectory-templates were used to filter out high-risk MCI subjects. Then, these subjects were inputted into the prognosis models which were constructed with different strategies for the two groups.

Results

Demographics. Table 1 shows the baseline demographic characteristics (age, gender, marital status, and education), genetic information (ApoEε4), clinical assessment scores (ADAS-13_bl, MMSE_bl, and the baseline of Clinical Dementia Rating Sum of Boxes (CDRSB_bl)), and trajectory label (ADAS-13 trajectory label, MMSE trajectory label) of subjects in two stages. Of the 85 subjects in stage I (trajectory dataset), 35 (41.2%) progressed to AD over the 3 years of follow-up, with the mean time to onset of AD being 20.4 ± 8.5 months (range 6.0–36.0 months). In stage II, 80 MCI subjects (21.4%) progressed to AD over 3 years, with the mean time to onset of AD being 20.4 ± 10.7 months (range 6.0–36.0 months).

Stage I: Trajectory modelling. K-means clustering based on ADAS-13 and MMSE separately generated two clusters, namely high-risk and low-risk (Fig. 1). Higher ADAS-13 scores and lower MMSE scores resulted in a higher risk of cognitive decline from MCI to AD. We used trajectory-templates to assign a trajectory label to the 374 patients according to the Euclidean proximity computed from all available time points.

Stage II: Performance of the MCI prognosis models. The subjects labelled with high-risk MCI were filtered out and may be prone to developing AD. Table 2 summarises the baseline characteristics and six change rate predictors in the first year of the high-risk MCI patients stratified by dementia status at 3 years. In the ADAS-13 predictive datasets, the groups with and without dementia differed significantly with respect to CDRSB_bl, ΔCDRSB, ΔHippocampus, ΔWholeBrain, but had similar distributions of age, sex, marital status, education, ApoEε4, MMSE_bl, ADAS-13_bl, Hippocampus_bl, WholeBrain_bl, Entorhinal_bl, ΔMMSE, ΔADAS-13, and

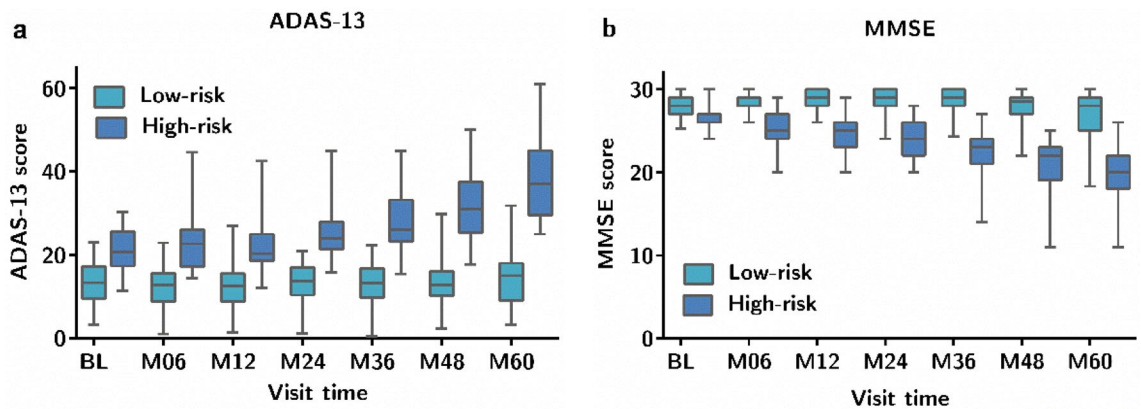


Figure 1. Clinical score distributions at each timepoint for the different trajectories derived from the K-means clustering (N = 85). The mean scores at each timepoint are used to build a template for each trajectory class. (a) Trajectory based on ADAS-13; (b) trajectory based on MMSE.

Characteristics	ADAS-13 predictive dataset (N = 110) Mean (SD) or N (%)		MMSE predictive dataset (N = 92) Mean (SD) or N (%)	
	No dementia (N = 44)	Dementia (N = 66)	No dementia (N = 35)	Dementia (N = 57)
Age (year)	74.3 (1.9)	71.9 (7.4)	75.1 (6.8)	72.6 (6.9)
Gender				
Male	27 (61.4)	35 (53.0)	22 (63.9)	33 (57.9)
Female	17 (38.6)	31 (47.0)	13 (37.1)	24 (42.1)
Marital status				
Married	34 (77.3)	53 (80.3)	28 (80.0)	47 (82.5)
Divorced	2 (4.5)	4 (6.1)	2 (5.7)	4 (7.0)
Others	8 (18.2)	9 (13.6)	5 (14.3)	6 (10.5)
Education				
Medium	0 (0.0)	0 (0.0)	0 (0.0)	0 (0.0)
High	44 (100.0)	66 (100.0)	35 (100.0)	57 (100.0)
ApoEε4				
Absent	21 (47.7)	21 (31.8)	13 (37.1)	17 (29.8)
Present	23 (52.3)	45 (68.2)	22 (62.9)	40 (70.2)
ADAS-13_bl	20.7 (4.0)	22.4 (5.4)	19.2 (5.0)	22.2 (6.0)*
MMSE_bl	27.6 (1.7)	27.1 (1.7)	26.5 (1.5)	26.7 (1.6)
CDRSB_bl	1.5 (0.8)	2.2(1.0)**	1.5 (0.8)	2.2 (0.9)*
Hippocampus_bl (cm ³)	6.4 (1.0)	6.4 (1.0)	6.5 (1.0)	6.4 (1.0)
WholeBrain_bl (cm ³)	1042.3(105.1)	1048.3(114.6)	1033.2(100.8)	1052.0 116.6)
Entorhinal_bl (cm ³)	3.5 (0.6)	3.3 (0.7)	3.5 (0.6)	3.3 (0.7)
ΔADAS-13	-0.2 (4.9)	2.4 (4.2)	-0.1 (5.9)	2.7 (4.6)
ΔMMSE	-1.3 (2.1)	-1.5 (1.9)	-1.1 (1.8)	-1.6 (1.9)*
ΔCDRSB	0.3 (0.8)	1.0(1.1) **	0.4 (0.9)	1.0 (1.1)*
ΔHippocampus (cm ³ /year)	-0.1 (0.3)	-0.3 (0.2) *	-0.2 (0.2)	-0.3 (0.2)*
ΔWholeBrain (cm ³ /year)	-5.4 (14.5)	-15.6 (10.8)**	-6.6 (15.8)	-15.8(11.6)*
ΔEntorhinal (cm ³ /year)	-0.1 (0.3)	-0.2 (0.3)	-0.1 (0.3)	-0.2 (0.3)

Table 2. Predictors of high-risk patients with MCI based on ADAS-13 (N = 110) and MMSE (N = 92) predictive datasets, stratified by dementia status over 3 years of follow-up. ADAS-13_bl, Alzheimer Disease Assessment Scale Cognitive 13 items at Baseline; MMSE_bl, Mini mental state examination at Baseline; CDRSB_bl, Clinical Dementia Rating Sum of Boxes at Baseline; ΔADAS-13, (ADAS-13_M12 – ADAS-13_bl)/1 year; ΔMMSE, (MMSE_M12 – MMSE_bl)/1 year; ΔCDRSB, (CDRSB_M12 – CDRSB_bl)/1 year; Hippocampus_bl, The Total Volumes of The Hippocampus at Baseline; WholeBrain_bl, Whole Brain at Baseline; Entorhinal_bl, Entorhinal Cortex at Baseline; ΔHippocampus, (Hippocampus_M12 – Hippocampus_bl)/1 year; ΔWholeBrain, (WholeBrain_M12 – WholeBrain_bl)/1 year; ΔEntorhinal, (Entorhinal_M12 – Entorhinal_bl)/1 year; SD, Standard deviation. ** $P < 0.001$; * $P < 0.05$.

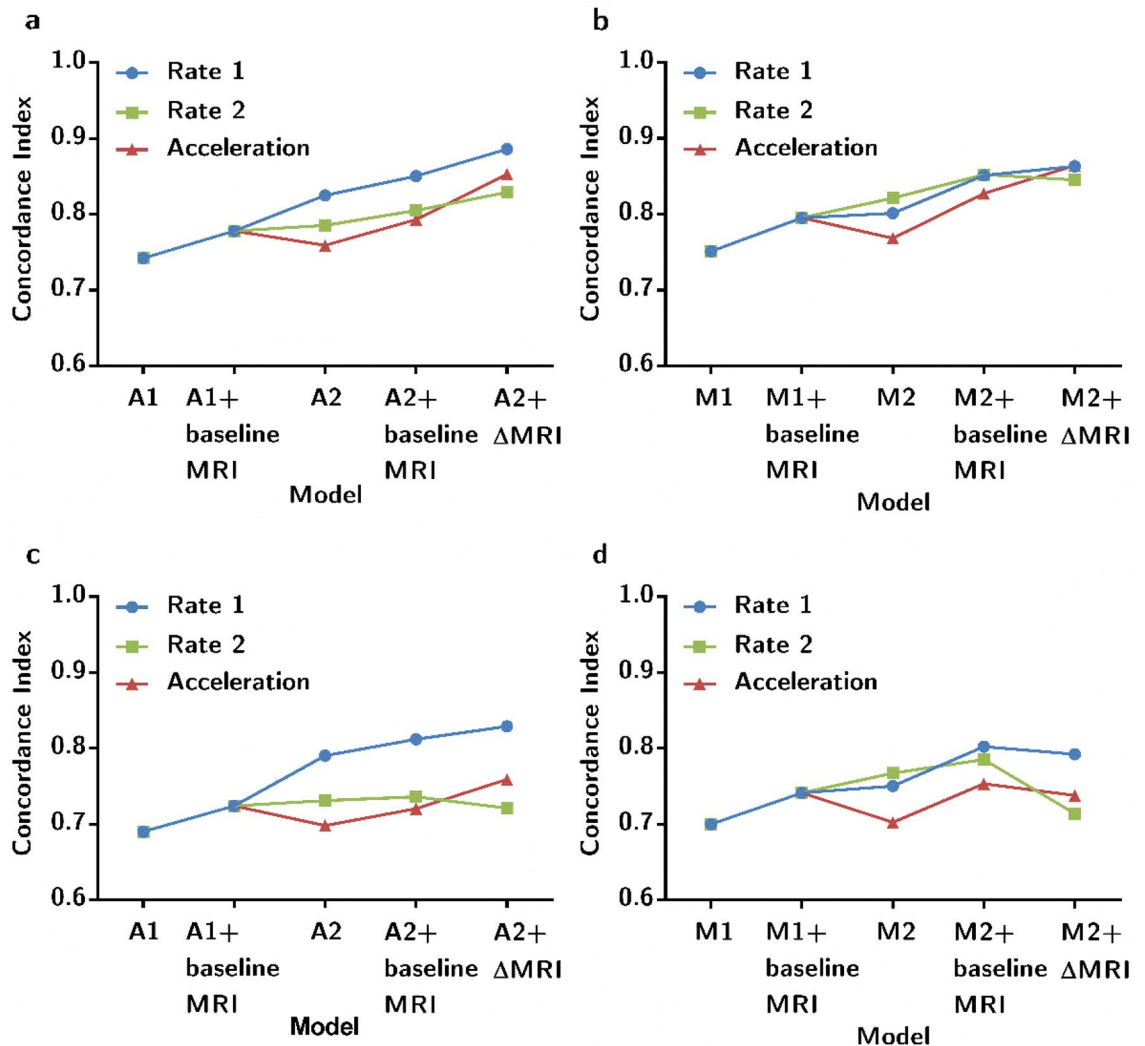


Figure 2. The concordance index (C-index) of models using different strategies to predict progression to dementia within 3 years. **(a)** The concordance index of ADAS-13 predictive dataset ($N = 110$); **(b)** the concordance index of MMSE predictive dataset ($N = 92$); **(c)** the concordance index of ADAS-13 predictive dataset by internet validation (bootstrap) ($N = 110$); **(d)** The concordance index of MMSE predictive dataset by internet validation (bootstrap) ($N = 92$).

Δ Entorhinal. In the MMSE predictive dataset, the groups with and without dementia were significantly different with respect to ADAS-13_bl and Δ MMSE, while the other results were consistent with those of the ADAS-13 predictive datasets.

Cox proportional hazards regression models were developed using all available data under different strategies for the 3-year progression to AD prediction. Five Cox models based on the ADAS-13 (MMSE) prediction dataset are shown in Supplementary Table S1 (Supplementary Table S2), with their hazard ratios and 95% confidence intervals (CIs).

For the ADAS-13 base model, we incorporated seven conventional risk factors into the baseline model A1 but found that only ADAS-13_bl was a significant predictor. The extended model A1+ baseline MRI with the addition of three baseline MRI measurements, and there were five significant predictors including age, marital status, CDRSB_bl, MMSE_bl, and ADAS-13_bl. As shown in Fig. 2, the concordance index (C-index) of model A1+ baseline MRI clearly increased with the inclusion of three baseline MRI measurements. Meanwhile, the NRI was 0.123 (95% CI 0.045, 0.664), indicating that the predictive performance of model A1+ baseline MRI improved by 12.3% compared to that of model A1 (Table 3). The IDI was 0.003, and the confidence interval included zero.

For the ADAS-13 longitudinal model, we added three change rates of clinical assessments in the longitudinal model A2, the significant variables were age, CDRSB_bl, ADAS-13_bl, Δ CDRSB, and Δ ADAS-13. A2+ baseline MRI included three baseline MRI imaging measurements based on A2, although these three neuroimaging variables were not significant in predicting the progression of MCI subjects, the discrimination performance of the A2+ baseline MRI was slightly improved as measured by the C-index. Similarly, three additional changes in MRI imaging measurements were incorporated into A2, resulting in six significant predictors in the model A2+ Δ MRI (age, CDRSB_bl, ADAS-13_bl, Δ CDRSB, Δ WholeBrain, and Δ Entorhinal). Figure 2 shows that the C-index

Predictive dataset	Prognosis model	NRI (95% CI)	IDI (95% CI)
ADAS-13 (N = 110)	A1+ baseline MRI versus A1	0.123 (0.045, 0.664)*	0.003 (-0.118, 0.093)
	A2+ baseline MRI versus A2	-0.062 (-0.074, 0.391)	0.006 (-0.172, 0.172)
	A2+ Δ MRI versus A2	0.246 (0.021, 0.848)*	0.090 (-0.094, 0.209)
MMSE (N = 92)	M1+ baseline MRI versus M1	0.177 (-0.035, 0.902)	0.008 (-0.085, 0.087)
	M2+ baseline MRI versus M2	0.201 (-0.046, 0.685)	0.005 (-0.148, 0.107)
	M2+ Δ MRI versus M2	0.489 (-0.132, 0.878)	0.065 (-0.062, 0.170)

Table 3. Performance of prognosis models among high-risk patients with MCI. A1, ADAS-13 baseline Prognosis Model; A2, ADAS-13 longitudinal Prognosis Model; M1, MMSE baseline Prognosis Model; M2, MMSE longitudinal Prognosis Model. ADAS-13, Alzheimer Disease Assessment Scale Cognitive 13 items; MMSE, Mini mental state examination; NRI, Net Reclassification Improvement; IDI, Integrated Discrimination Improvement. Values based on the following assumptions: Risk of event = 10%. *The indices are statistically significant.

of model A2+ Δ MRI was the highest, and it slightly increased with the inclusion of three change values of MRI imaging measurements compared to A2. Meanwhile, the NRI was 0.246 (95% CI 0.021, 0.848), and the IDI was 0.090 (95% CI -0.094, 0.209). This indicated that the predictive performance of model A2+ Δ MRI improved by 24.6% compared to that of model A2 (Table 3) by NRI. We undertook internal validation by bootstrap, and the longitudinal model A2+ Δ MRI had the best discrimination performance (Optimism-corrected c-index = 0.830) (Supplementary Table S3).

For the MMSE base model, the Cox model was built using a similar strategy. As shown in Fig. 2, the extended model M1+ baseline MRI clearly increased with the inclusion of three baseline MRI measurements. Both the NRI and IDI indices were positive, but the confidence interval included zero.

For the MMSE longitudinal model, the C-index of the extended model M2+ baseline MRI with additional three baseline MRI imaging measurements increased significantly (Fig. 2). Both the NRI and IDI indices were positive, although the confidence interval did not include zero (Table 3). Figure 2 shows that the C-index of model M2+ baseline MRI was the highest. It did not increase with the inclusion of three change rates of MRI measurements in the validation of the data. Meanwhile, the longitudinal model M2+ baseline MRI validated by bootstrap had the best discrimination performance (Optimism-corrected c-index = 0.802) (Supplementary Table S3).

Moreover, to compare the change rate in the first year, we also computed for the cognitive decline rate in the second year and acceleration in the first 2 years (Fig. 2). The Cox model incorporating the change rate in the first year had the best predictive performance, except for M2. A2+ Δ MRI, including the change rates of clinical assessment scores and MRI measurements, showed the best performance of the prognosis model for patients with MCI.

Discussion

In this study, we constructed and validated a two-stage screening frame for subjects with MCI at an increased risk of developing AD in 3 years.

Previous studies have indicated that clinical assessment tests are excellent at predicting patients with MCI progressing to AD and should be a critical component of identifying AD at the prodementia stage¹⁹. In addition, there was a significant improvement in classifying MCI that were at risk using the duration of follow-up²⁰. We enrolled subjects assessed by clinical assessments at seven time points over 5 years to characterise the MCI progression trajectory.

Considering the heterogeneity of MCI progression, we chose two clusters for the ADAS-13 and MMSE. The clustering yielded two groups, namely the high-risk and low-risk group, which reflected the different risks of progression to AD (see Fig. 3). The number of clusters depended not only on the data-driven approach but also on the desired specificity of the trajectory. Higher ADAS-13 scores and lower MMSE scores indicate a higher risk of conversion to AD²¹. Trajectory labels were used to filter out high-risk patients with MCI. Several studies have utilised hierarchical clustering to identify target populations, but they considered trajectory labels as the goal of the predictive task^{22–24}. This strategy has three advantages. First, the trajectory labels characterised the progression of MCI without being restricted by strict cut-offs, defining a specific time window. Second, the trajectory-templates could assign a trajectory label for subjects with missing follow-up data²²; in other words, the technique provides a method for solving the problem of missing time points in a longitudinal study. Third, the trajectory labels can be used to predict the risk of AD onset at an individual level and provide a screening strategy for high-risk patients with MCI²⁵. This may have useful clinical implications for more precise disease management and personalised interventions.

Considering the two different progression trajectories of MCI, we filtered out high-risk patients who tended to develop cognitive decline and may progress to AD in the future. Cox models were developed to evaluate the value of additional MRI measurements for a 3-year prognosis model. The results imply that models with additional MRI measurements could improve predictive performance. Therefore, high-risk patients with MCI should be recommended for a follow-up MRI 1 year later. Several studies have evaluated the predictive utility of prognostic markers, but only focused on baseline measurements¹⁵. One study developed a joint modelling of longitudinal markers and a time-to-event data method to evaluate the effects of longitudinal markers. However, this method only analysed each marker independently¹⁸. We transformed the longitudinal predictors for change

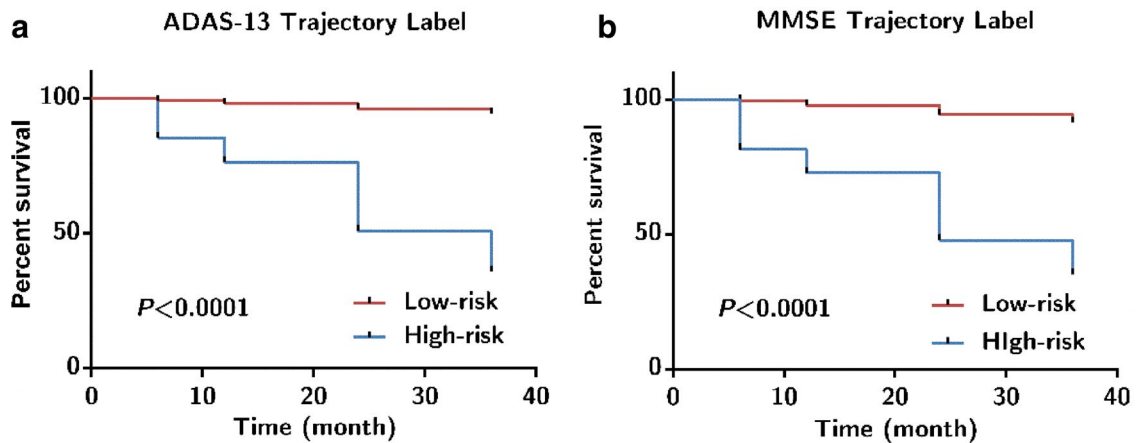


Figure 3. Kaplan–Meier curves for 3-year progression to AD in MCI based on ADAS-13 (N = 110) and MMSE (N = 92) predictive dataset. (a) ADAS-13 Trajectory Label; (b) MMSE Trajectory Label.

rate and constructed base and longitudinal prognosis models including multiple predictors for different clinical application scenarios.

In the current study, the predictive performance of the baseline model (A1, A1+ baseline MRI) was lower than that of the longitudinal model (A2, A2+ baseline MRI, and A2+ Δ MRI) according to the C-index (see Fig. 2). Similarly, the predictive performance of the baseline model (M1, M1+ baseline MRI) was lower than that of the longitudinal model (M2+ baseline MRI, M2+ Δ MRI) (see Fig. 2). As CDRSB_bl did not satisfy the proportional hazards assumption in models A1, M1, and M2, we translated the continuous variable CDRSB_bl into the categorical variable (CDRSB_bl1) using X-tile software. The stratified Cox models were then performed using CDRSB_bl1 in models A1, M1, and M2 and by marital status in A2.

Overall, the ADAS-13 longitudinal model has better performance than that of MMSE. The results indicate that ADAS-13 is more sensitive in classifying patients with MCI and filtering out high-risk individuals. Furthermore, the A2+ Δ MRI model had the best predictive performance for progression to AD among high-risk patients with MCI. There were six significant variables in A2+ Δ MRI, including age, CDRSB_bl, ADAS-13_bl, Δ CDRSB, Δ WholeBrain, and Δ Entorhinal. We computed the change rate in the first year simply and avoided the longitudinal variables that needed complex technology. Meanwhile, it is helpful to find an interpretable marker in the early stage. In model A2+ Δ MRI, Δ WholeBrain and Δ Entorhinal significantly improved the predictive performance for AD over a 3-year follow-up. Several studies have also shown that atrophy estimates in characteristically vulnerable brain regions, such as the hippocampus and entorhinal cortex, reflect the disease stage and are predictive of progression of MCI to AD²⁶.

Here, we propose a two-stage screening framework for MCI subjects facing the risk of AD. The trajectory-template could classify the subjects with MCI into high-risk and low-risk groups at the individual level. When an individual with MCI is predicted to be high-risk, more assessments and additional MRI 1 year later and personalised interventions would be recommended by the clinician. Otherwise, low-risk MCI subjects should be considered for regular clinical assessment. The goal of prognosis models is to provide a simple and accurate tool to forecast the risk of high-risk patients progressing to AD in 3 years²⁷. In short, this strategy could facilitate decision-making pertaining to the frequency and monitoring methods that should be conducted in MCI individuals^{12,28}. Additionally, it also saves multiple medical resources and reduces the patient's burden.

This study has some limitations. First, the ADNI cohorts may not represent the general population, and most of the subjects were well-educated. Next, because of the two-stage design of the screening frame, only high-risk patients were filtered out according to the trajectory labels. Because of the small sample size used for prognosis models, we ran the analyses on the entire sample, instead of splitting the sample into training and testing datasets²⁹. However, the performance of the prognosis models was evaluated via internal validation (bootstrap method). Bootstrapping is an attractive method for internal validation, and it uses the entire dataset for model development and provides nearly unbiased estimates of predictive accuracy³⁰. Whether MRI enhances prediction in other dementia risk models requires further independent validation. Finally, we did not consider the specific money and time saved using this method, but this is our future work.

The key strength of this study is that it is a two-stage screening strategy for MCI patients, which is likely to have clinical utility and save on medical resources. In future studies, we may explore additional MRI clinical application scenarios for different targeting populations.

In conclusion, the study indicated that follow-up MRI examination is recommended 1 year after identification for high-risk patients, and regular clinical cognitive assessments for low-risk MCI patients, especially considering limited medical and financial resources. We believe that this work will further motivate the exploration of multimodal longitudinal prognosis models, which will improve prognostic predictions in MCI.

Materials and methods

Datasets and subjects. The data used in this study were downloaded from the Alzheimer's Disease Neuroimaging Initiative (ADNI) database (<http://adni.loni.usc.edu/>). The ADNI was launched in 2003, and the primary goal of ADNI was to test whether serial clinical assessments, neuropsychological assessments, MRI, PET, and other biological markers can be combined to measure the progression of MCI and early AD. Detailed information regarding the ADNI study procedures, including participant inclusion and exclusion criteria, can be found at <http://www.adni-info.org>. As part of the ADNI, subjects with MCI were assessed using the ADAS-13 and MMSE at baseline and at 6, 12, 24, 36, 48, and 60 months. For stage I modelling, 85 ADNI-1 subjects with MCI were included in the trajectory dataset, which was used to build trajectory-templates of cognitive decline. For stage II, 374 subjects with MCI from ADNI GO/2 with two clinical assessments in at least four time points over 5 years were assigned trajectory labels. MCI subjects labelled as high-risk were filtered out and included in the predictive dataset. The ADNI was approved by the institutional review board of each participating site. All participants provided written informed consent. For more information, see <http://www.adni-info.org>. This study was approved by the ethics committee of Shanxi Medical University. All methods were carried out in accordance with relevant guidelines and regulation. We considered all these subjects as MCI patients in our analysis. The criteria for MCI diagnosis were the same as those defined by Hojjati et al.³¹.

Measures. In the present study, the potential prognostic factors were clinical assessment and MRI measurements at baseline and their change rate in the first year. The Alzheimer Disease Assessment Scale Cognitive (ADAS-Cog) is a widely used clinical assessment tool for evaluating the cognitive characteristics of AD. The ADAS-13 is the total score of 13 items ranging from 0 to 85, with higher scores indicating poorer cognitive function. The MMSE includes 11 questions with scores ranging from 0 to 30, with lower scores reflecting more severe cognitive impairment¹⁰. The Clinical Dementia Rating Scale (CDR) is widely used for the detection and severity classification of AD. We usually calculated the Clinical Dementia Rating Sum of Boxes (CDRSB) ranging from 0 to 18, with higher scores indicating more severe dementia^{32,33}. Evidence supports the usefulness of CDR in detecting MCI and dementia. CDR should be considered for staging cognitive impairment in at-risk populations³⁴. Three structural MRI measurements associated with cognitive decline and dementia, the total volumes of the hippocampus, whole brain, and entorhinal cortex were selected for analysis^{29,35}. The details of the MRI protocols used to acquire the image datasets in the ADNI project can be found at <http://adni.loni.usc.edu/methods/documents/>. Demographic data and apolipoprotein E (ApoE) ϵ 4 allele status (present or absent) were collected at the baseline visit.

Stage I: Trajectory modelling. The progression trajectory was characterised using multiple-timepoint clinical assessment scores, including the ADAS-13 and MMSE scales^{22,36}. The trajectory dataset was used as the input for K-means clustering. The Euclidean distance between the longitudinal clinical assessment score vectors was used as a similarity metric, and Ward's method was used as a linkage criterion for clustering. The average clinical assessment scores from each cluster at each time point were used as trajectory templates for each class.

Stage II: Construction and evaluation of the MCI prognosis models. The trajectory template was used to assign a trajectory label for the 374 ADNI-GO/2 MCI subjects. High-risk MCI subjects were filtered out according to the ADAS-13 and MMSE trajectories ($n = 110$ and 92 , respectively). To evaluate the benefit of MRI measurements for predicting the conversion of MCI, we developed 3-year survival models using high-risk patients. The main outcome of the prognosis model was AD that was first diagnosed during follow-up. Multivariate models were calculated using the Cox proportional hazards regression analysis. The proportional hazards assumption was tested in R, and the variable that did not satisfy the assumption was input into the model as a stratified variable. For convenience, the first letter of the ADAS-13 and MMSE was used to distinguish between the two different predictive datasets. The abbreviations are used to represent the different prognosis models. Models A1 and A2 indicate baseline and longitudinal models for ADAS-13, while Models M1 and M2 indicate baseline and longitudinal models for MMSE. The extended models were renamed according to the increased variables compared to the baseline and longitudinal models (Table 4). Considering the longitudinal nature, we computed the change rate of clinical assessment scores (Δ ADAS-13, Δ MMSE, and Δ CDRSB) and MRI measurements (Δ Hippocampus, Δ WholeBrain, and Δ Entorhinal) in the first year. For example, we defined the Δ CDRSB as follows: Δ CDRSB = (CDRSB_M12 - CDRSB_bl)/1 year (with “_M12” indicating the 12th month, with “_bl” indicating baseline). To compare the change rate in the first year (rate 1), the change rate in the second year (rate 2) and acceleration in the first 2 years (acceleration) were also computed.

The C-index was calculated for the comparison of different models, which is commonly used to evaluate the discriminative abilities of Cox models^{37,38}. Additionally, we evaluated the improvements in discriminating ability attained with the extended models in comparison with the basic model by the net reclassification improvement (NRI; with cut = 10%)³⁷, and the integrated discrimination improvement (IDI)^{39–41}.

Statistical analyses. The categorical variables in the present study were recorded as follows: gender (1: male, 2: female), marital status (1: married, 2: divorced, 3: others), education (1: medium (years of education < 12), 2: high (years of education ≥ 12)), and ApoE4 (1: absent, 2: present).

Differences in demographic characteristics were tested using the chi-square test (for categorical variables), one-way analysis of variance (for continuous normally distributed variables), or the Kruskal–Wallis test (for continuous, non-normally distributed variables). X-tile software (version 3.6.1; Yale University School of Medicine, New Haven, CT, USA) was applied to the X-tile plots. An optimum cut-off was automatically selected by an approach provided by X-tile plots, and it was based on the highest chi-square statistic defined using the log-rank

Prognosis models	Predictors
Baseline	
A1/M1	Age, gender, marital status, ApoE ϵ 4, ADAS-13_bl, MMSE_bl, and CDRSB_bl
A1+ baseline MRI/M1+ baseline MRI	A1/M1+ Hippocampus_bl, WholeBrain_bl, and Entorhinal_bl
Longitudinal	
A2/M2	Age, gender, marital status, ApoE ϵ 4, ADAS-13_bl, MMSE_bl, CDRSB_bl, Δ ADAS-13, Δ MMSE, and Δ CDRSB
A2+ baseline MRI/M2+ baseline MRI	A2/M2+ Hippocampus_bl, WholeBrain_bl, and Entorhinal_blc
A2+ Δ MRI/M2+ Δ MRI	A2/M2+ Δ Hippocampus, Δ WholeBrain, and Δ Entorhinal

Table 4. The prognosis models and the corresponding predictors for ADAS-13 (N = 110) and MMSE (N = 92) predictive dataset. A1, ADAS-13 baseline Prognosis Model; A2, ADAS-13 longitudinal Prognosis Model; M1, MMSE baseline Prognosis Model; M2, MMSE longitudinal Prognosis Model; ADAS-13_bl, Alzheimer Disease Assessment Scale Cognitive 13 items at Baseline; MMSE_bl, Mini mental state examination at Baseline; CDRSB_bl, Clinical Dementia Rating Sum of Boxes at Baseline; Hippocampus_bl, The Total Volumes of The Hippocampus at Baseline; WholeBrain_bl, Whole Brain at Baseline; Entorhinal_bl, Entorhinal Cortex at Baseline; Δ ADAS-13, (ADAS-13_M12 – ADAS-13_bl)/1 year; Δ MMSE, (MMSE_M12 – MMSE_bl)/1 year; Δ CDRSB, (CDRSB_M12 – CDRSB_bl)/1 year; Δ Hippocampus, (Hippocampus_M12 – Hippocampus_bl)/1 year; Δ WholeBrain, (WholeBrain_M12 – WholeBrain_bl)/1 year; Δ Entorhinal, (Entorhinal_M12 – Entorhinal_bl)/1 year.

test and Kaplan–Meier survival analysis. To correct for optimism bias in the C-index, we undertook internal validation using 500 bootstrap samples^{30,42,43}. All other statistical analyses were performed using SPSS 25.0 and R version 3.6.1. The R packages used in this study included survival, pec, and rms. GraphPad Prism 6 software was used to plot the data. A two-sided $P < 0.05$, was considered to indicate a significant difference.

Data availability

The data analyzed in the study are available from the ADNI website. (<http://adni.loni.usc.edu>).

Received: 31 August 2020; Accepted: 18 August 2021

Published online: 02 September 2021

References

- Rathore, S., Habes, M., Iftikhar, M. A., Shacklett, A. & Davatzikos, C. A review on neuroimaging-based classification studies and associated feature extraction methods for Alzheimer's disease and its prodromal stages. *Neuroimage* **155**, 530–548. <https://doi.org/10.1016/j.neuroimage.2017.03.057> (2017).
- Petersen, R. C. *et al.* Mild cognitive impairment: A concept in evolution. *J. Intern. Med.* **275**, 214–228. <https://doi.org/10.1111/joim.12190> (2014).
- Petersen, R. C. *et al.* Mild cognitive impairment: Clinical characterization and outcome. *Arch. Neurol.* **56**, 303–308. <https://doi.org/10.1001/archneur.56.3.303> (1999).
- Eshkoor, S. A., Hamid, T. A., Mun, C. Y. & Ng, C. K. Mild cognitive impairment and its management in older people. *Clin. Interv. Aging* **10**, 687–693. <https://doi.org/10.2147/CIA.S73922> (2015).
- Ezzati, A. *et al.* Optimizing machine learning methods to improve predictive models of Alzheimer's disease. *J. Alzheimers Dis.* **71**, 1027–1036. <https://doi.org/10.3233/JAD-190262> (2019).
- Liu, X. *et al.* Use of multimodality imaging and artificial intelligence for diagnosis and prognosis of early stages of Alzheimer's disease. *Transl. Res.* **194**, 56–67. <https://doi.org/10.1016/j.trsl.2018.01.001> (2018).
- Zhang, D. *et al.* Multimodal classification of Alzheimer's disease and mild cognitive impairment. *Neuroimage* **55**, 856–867. <https://doi.org/10.1016/j.neuroimage.2011.01.008> (2011).
- Arevalo-Rodriguez, I. *et al.* Mini-Mental State Examination (MMSE) for the detection of Alzheimer's disease and other dementias in people with mild cognitive impairment (MCI). *Cochrane Database Syst. Rev.* **3**, CD010783. <https://doi.org/10.1002/14651858.CD010783.pub2> (2015).
- Qin, Y. *et al.* Risk classification for conversion from mild cognitive impairment to Alzheimer's disease in primary care. *Psychiatry Res.* **278**, 19–26. <https://doi.org/10.1016/j.psychres.2019.05.027> (2019).
- Wu, Y. *et al.* Predicting Alzheimer's disease based on survival data and longitudinally measured performance on cognitive and functional scales. *Psychiatry Res.* **291**, 113201. <https://doi.org/10.1016/j.psychres.2020.113201> (2020).
- Moll van Charante, E. P. *et al.* Effectiveness of a 6-year multidomain vascular care intervention to prevent dementia (preDIVA): A cluster-randomised controlled trial. *Lancet* **388**, 797–805. [https://doi.org/10.1016/S0140-6736\(16\)30950-3](https://doi.org/10.1016/S0140-6736(16)30950-3) (2016).
- Sommerlad, A. & Livingston, G. Preventing Alzheimer's dementia. *BMJ* **359**, j5667. <https://doi.org/10.1136/bmj.j5667> (2017).
- Tang, E. Y. *et al.* Current developments in dementia risk prediction modelling: An updated systematic review. *PLoS ONE* **10**, e0136181. <https://doi.org/10.1371/journal.pone.0136181> (2015).
- Yassine, H. N. Targeting prodromal Alzheimer's disease: Too late for prevention? *Lancet Neurol.* **16**, 946–947. [https://doi.org/10.1016/S1474-4422\(17\)30372-1](https://doi.org/10.1016/S1474-4422(17)30372-1) (2017).
- Barnes, D. E. *et al.* A point-based tool to predict conversion from mild cognitive impairment to probable Alzheimer's disease. *Alzheimers Dement* **10**, 646–655. <https://doi.org/10.1016/j.jalz.2013.12.014> (2014).
- Kong, D. *et al.* Predicting Alzheimer's disease using combined imaging-whole genome SNP data. *J. Alzheimers Dis.* **46**, 695–702. <https://doi.org/10.3233/JAD-150164> (2015).
- Melis, R. J. F., Haaksma, M. L. & Muniz-Terrera, G. Understanding and predicting the longitudinal course of dementia. *Curr. Opin. Psychiatry* **32**, 123–129. <https://doi.org/10.1097/YCO.0000000000000482> (2019).
- Li, K. *et al.* Prediction of conversion to Alzheimer's disease with longitudinal measures and time-to-event data. *J. Alzheimers Dis.* **58**, 361–371. <https://doi.org/10.3233/JAD-161201> (2017).

19. Belleville, S. *et al.* Neuropsychological measures that predict progression from mild cognitive impairment to Alzheimer's type dementia in older adults: A systematic review and meta-analysis. *Neuropsychol. Rev.* **27**, 328–353. <https://doi.org/10.1007/s11065-017-9361-5> (2017).
20. Moscoso, A. *et al.* Prediction of Alzheimer's disease dementia with MRI beyond the short-term: Implications for the design of predictive models. *Neuroimage Clin.* **23**, 101837. <https://doi.org/10.1016/j.nicl.2019.101837> (2019).
21. Song, Y. N. *et al.* Risk factors of rapid cognitive decline in Alzheimer's disease and mild cognitive impairment: A systematic review and meta-analysis. *J. Alzheimers Dis.* **66**, 497–515. <https://doi.org/10.3233/JAD-180476> (2018).
22. Bhagwat, N., Viviano, J. D., Voineskos, A. N., Chakravarty, M. M. & Alzheimer's Disease Neuroimaging, I. Modeling and prediction of clinical symptom trajectories in Alzheimer's disease using longitudinal data. *PLoS Comput. Biol.* **14**, e1006376. <https://doi.org/10.1371/journal.pcbi.1006376> (2018).
23. Cleret de Langavant, L., Bayen, E. & Yaffe, K. Unsupervised machine learning to identify high likelihood of dementia in population-based surveys: Development and validation study. *J. Med. Internet Res.* **20**, e10493. <https://doi.org/10.2196/10493> (2018).
24. Edmonds, E. C. *et al.* Early versus late MCI: Improved MCI staging using a neuropsychological approach. *Alzheimers Dement* **15**, 699–708. <https://doi.org/10.1016/j.jalz.2018.12.009> (2019).
25. Pellegrini, M., Zoghi, M. & Jaberzadeh, S. Cluster analysis and subgrouping to investigate inter-individual variability to non-invasive brain stimulation: A systematic review. *Rev. Neurosci.* **29**, 675–697. <https://doi.org/10.1515/revneuro-2017-0083> (2018).
26. Frisoni, G. B., Fox, N. C., Jack, C. R. Jr., Scheltens, P. & Thompson, P. M. The clinical use of structural MRI in Alzheimer disease. *Nat. Rev. Neurol.* **6**, 67–77. <https://doi.org/10.1038/nrneuro.2009.215> (2010).
27. Cooper, B. Epidemiology in a changing world: Implications for population-based research on mental disorders. *Epidemiol. Psychiatr. Sci.* **23**, 141–146. <https://doi.org/10.1017/S2045796013000644> (2014).
28. Andrieu, S. *et al.* Effect of long-term omega 3 polyunsaturated fatty acid supplementation with or without multidomain intervention on cognitive function in elderly adults with memory complaints (MAPT): A randomised, placebo-controlled trial. *Lancet Neurol.* **16**, 377–389. [https://doi.org/10.1016/S1474-4422\(17\)30040-6](https://doi.org/10.1016/S1474-4422(17)30040-6) (2017).
29. Stephan, B. C. *et al.* Usefulness of data from magnetic resonance imaging to improve prediction of dementia: Population based cohort study. *BMJ* **350**, h2863. <https://doi.org/10.1136/bmj.h2863> (2015).
30. Harrell, F. E. Jr., Lee, K. L. & Mark, D. B. Multivariable prognostic models: Issues in developing models, evaluating assumptions and adequacy, and measuring and reducing errors. *Stat. Med.* **15**, 361–387. [https://doi.org/10.1002/\(SICI\)1097-0258\(19960229\)15:4%3c361::AID-SIM168%3e3.0.CO;2-4](https://doi.org/10.1002/(SICI)1097-0258(19960229)15:4%3c361::AID-SIM168%3e3.0.CO;2-4) (1996).
31. Hojjati, S. H., Ebrahimzadeh, A., Khazae, A., Babajani-Feremi, A. & Alzheimer's Disease Neuroimaging, I. Predicting conversion from MCI to AD using resting-state fMRI, graph theoretical approach and SVM. *J. Neurosci. Methods* **282**, 69–80. <https://doi.org/10.1016/j.jneumeth.2017.03.006> (2017).
32. Barca, M. L. *et al.* Trajectories of depressive symptoms and their relationship to the progression of dementia. *J. Affect. Disord.* **222**, 146–152. <https://doi.org/10.1016/j.jad.2017.07.008> (2017).
33. Lima, A. P. V., Castilhos, R. & Chaves, M. L. F. The use of the clinical dementia rating scale sum of boxes scores in detecting and staging cognitive impairment/dementia in Brazilian patients with low educational attainment. *Alzheimer Dis. Assoc. Disord.* **31**, 322–327. <https://doi.org/10.1097/WAD.000000000000205> (2017).
34. Huang, H. C., Tseng, Y. M., Chen, Y. C., Chen, P. Y. & Chiu, H. Y. Diagnostic accuracy of the Clinical Dementia Rating Scale for detecting mild cognitive impairment and dementia: A bivariate meta-analysis. *Int. J. Geriatr. Psychiatry* **36**, 239–251. <https://doi.org/10.1002/gps.5436> (2021).
35. Devanand, D. P. *et al.* Hippocampal and entorhinal atrophy in mild cognitive impairment: Prediction of Alzheimer disease. *Neurology* **68**, 828–836. <https://doi.org/10.1212/01.wnl.0000256697.20968.d7> (2007).
36. Verlinden, V. J. A. *et al.* Trajectories of decline in cognition and daily functioning in preclinical dementia. *Alzheimers Dement* **12**, 144–153. <https://doi.org/10.1016/j.jalz.2015.08.001> (2016).
37. Fisher, L. D. & Lin, D. Y. Time-dependent covariates in the Cox proportional-hazards regression model. *Annu. Rev. Public Health* **20**, 145–157. <https://doi.org/10.1146/annurev.publhealth.20.1.145> (1999).
38. Moolgavkar, S. H., Chang, E. T., Watson, H. N. & Lau, E. C. An assessment of the Cox proportional hazards regression model for epidemiologic studies. *Risk Anal.* **38**, 777–794. <https://doi.org/10.1111/risa.12865> (2018).
39. Alba, A. C. *et al.* Discrimination and calibration of clinical prediction models: Users' guides to the medical literature. *JAMA* **318**, 1377–1384. <https://doi.org/10.1001/jama.2017.12126> (2017).
40. Desikan, R. S. *et al.* Genetic assessment of age-associated Alzheimer disease risk: Development and validation of a polygenic hazard score. *PLoS Med.* **14**, e1002258. <https://doi.org/10.1371/journal.pmed.1002258> (2017).
41. Steyerberg, E. W. *et al.* Assessing the performance of prediction models: A framework for traditional and novel measures. *Epidemiology* **21**, 128–138. <https://doi.org/10.1097/EDE.0b013e3181c30fb2> (2010).
42. Steyerberg, E. W. *Clinical Prediction Models* 90–97 (Springer, 2009).
43. Fusar-Poli, P., Hijazi, Z., Stahl, D. & Steyerberg, E. W. The science of prognosis in psychiatry: A review. *JAMA Psychiatr.* **75**, 1289–1297. <https://doi.org/10.1001/jamapsychiatry.2018.2530> (2018).

Acknowledgements

This work was supported by the National Natural Science Foundation of China [81973154, 81673277, and 81903418]. Data used in this article were obtained from the Alzheimer's Disease Neuroimaging Initiative (ADNI) database (adni.loni.usc.edu). As such, the investigators within the ADNI contributed to the design and implementation of ADNI and/or provided data but did not participate in the analysis or writing of this report. A complete listing of ADNI investigators can be found at: http://adni.loni.usc.edu/wp-content/uploads/how_to_apply/ADNI_Acknowledgement_List.pdf. Data collection and sharing for this project was funded by the Alzheimer's Disease Neuroimaging Initiative (ADNI) (National Institutes of Health Grant U01 AG024904) and DOD ADNI (Department of Defense award number W81XWH-12-2-0012). ADNI is funded by the National Institute on Aging, the National Institute of Biomedical Imaging and Bioengineering, and through generous contributions from the following: AbbVie, Alzheimer's Association; Alzheimer's Drug Discovery Foundation; Araclon Biotech; BioClinica, Inc.; Biogen; Bristol-Myers Squibb Company; CereSpir, Inc.; Cogstate; Eisai Inc.; Elan Pharmaceuticals, Inc.; Eli Lilly and Company; EuroImmun; F. Hoffmann–La Roche Ltd and its affiliated company Genentech, Inc.; Fujirebio; GE Healthcare; IXICO Ltd.; Janssen Alzheimer Immunotherapy Research & Development, LLC.; Johnson & Johnson Pharmaceutical Research & Development LLC.; Lumosity; Lundbeck; Merck & Co., Inc.; Meso Scale Diagnostics, LLC.; NeuroRx Research; Neurotrack Technologies; Novartis Pharmaceuticals Corporation; Pfizer Inc.; Piramal Imaging; Servier; Takeda Pharmaceutical Company; and Transition Therapeutics. The Canadian Institutes of Health Research is providing funds to support ADNI clinical sites in Canada. Private sector contributions are facilitated by the Foundation for the National Institutes of Health (www.fnih.org). The grantee organization is the Northern California Institute for Research and Education, and the study is coordinated by the

Alzheimer's Therapeutic Research Institute at the University of Southern California. ADNI data are disseminated by the Laboratory for Neuro Imaging at the University of Southern California.

Author contributions

H.-M.Y. raised new questions and ideas regarding this article. X.-Y.G. performed the statistical analyses and wrote the manuscript. K.C. and L.L. contributed to the study design and critical revisions. Y.Q. and Y.-H.L. contributed to the interpretation of the data and revised the manuscript. J.C. and H.-J.H. contributed to the data acquisition and management. All authors reviewed the manuscript.

Competing interests

The authors declare no competing interests.

Additional information

Supplementary Information The online version contains supplementary material available at <https://doi.org/10.1038/s41598-021-96914-3>.

Correspondence and requests for materials should be addressed to H.-M.Y.

Reprints and permissions information is available at www.nature.com/reprints.

Publisher's note Springer Nature remains neutral with regard to jurisdictional claims in published maps and institutional affiliations.



Open Access This article is licensed under a Creative Commons Attribution 4.0 International License, which permits use, sharing, adaptation, distribution and reproduction in any medium or format, as long as you give appropriate credit to the original author(s) and the source, provide a link to the Creative Commons licence, and indicate if changes were made. The images or other third party material in this article are included in the article's Creative Commons licence, unless indicated otherwise in a credit line to the material. If material is not included in the article's Creative Commons licence and your intended use is not permitted by statutory regulation or exceeds the permitted use, you will need to obtain permission directly from the copyright holder. To view a copy of this licence, visit <http://creativecommons.org/licenses/by/4.0/>.

© The Author(s) 2021